Optimization of lithium target for epithermal neutrons generation

B. Bayanov, V. Belov, V. Kindyuk[b], S. Taskaev

Budker Institute of Nuclear Physics, Novosibirsk, Russia

[b] *Novosibirsk State University, Novosibirsk, Russia*

Pilot innovative accelerator based neutron source for neutron capture therapy is under construction now at the Budker Institute of Nuclear Physics, Novosibirsk, Russia. One of the main elements of the facility is lithium target, that produces neutrons via threshold ^{7}Li(p,n)^{7}Be reaction at 25 kW proton beam with energies 1.915 MeV or 2.5 MeV.

In the present report, the results of experiments on neutron producing target prototype are presented, the results of calculations of hydraulic resistance for heat carrier flow and lithium layer temperature are shown. Calculation showed that the lithium target could run up to 10 mA proton beam before melting. Choice of target variant is substantiated. Program of immediate necessary experiments is described. Target design for neutron source constructed at BINP is presented.

1. Introduction

The Budker Institute of Nuclear Physics and the Institute of Physics and Power Engineering, Obninsk, have proposed an accelerator based neutron source for neutron capture and fast neutron therapy at hospital (Bayanov, 1998). Innovative approach is based upon tandem electrostatic accelerator with vacuum insulation and near threshold neutron generation. Pilot facility is under construction now at the Budker Institute of Nuclear Physics. One of the main elements of the facility is lithium target producing neutrons via threshold ^{7}Li(p,n)^{7}Be reaction at 25 kW proton beam.

Lithium targets for two modes of neutron beam production are developed. The first one provides kinematically collimated neutrons via near-threshold ^{7}Li(p,n)^{7}Be reaction at proton energies of 1.915 MeV. Target will be created as a 2 – 3 μm thick lithium layer on the surface of disk cooled. In the second mode, therapeutically useful orthogonal neutron beams are produced at proton energy of 2.5 MeV. 100 μm thick lithium target is needed in this case.

The main problems of lithium neutron producing target are heat removal, lithium evaporation, radiation blistering, and radioactive ^{7}Be isotope. The main requirement for the target cooling is to maintain the temperature of lithium layer below 300 °C (Bayanov, 1998), or better below the lithium melting temperature 182 °C. Liquid metal heat carrier (gallium) is preferable than water as there is no 100 °C limit on temperature of a surface being cooled, and there is no danger in case of coolant leakage into vacuum volume. However, higher pressure drop on cooling channels is needed, and liquid metal heat carrier has very chemical activity.

In the present report, choice of target for the source under construction is substantiated, the necessary experiments are shown, and the conception of the target is presented.

2. Neutron target prototype design

The first model of neutron producing stationary target was made (Belov, 2000) and tested under 20 kW 1.4 MeV electron beam (Belov, 2002). This target consisted of molybdenum plate 64 mm in diameter, 0.2 mm thick that diffusely welded on an ARMCO steel disk 74 mm in diameter, 4 mm thick. Ten rectangular grooves were on the disk for cooling. In the process of examination, heat removal up to 650 W cm^{-2} was provided using water, and liquid metal cooling resulted in the target destruction due to high chemical interaction of gallium with ARMCO steel.

These experiments and calculations showed the way to improve the target and cooling system. A new variant of target is presented in Fig. 1. It is a tungsten disk 80 mm in diameter, 3 mm thick with thirteen cooling rectangular channels 3 mm × 2 mm, 45 to 64 mm length, at an interval of 3.7 mm, pressed to titanium body without diffuse welding. Laborious diffuse welding was refused, which resulted in possibility to obtain more homogeneous temperature field on the surface of the target at the expense of decrease (from 1.5 mm to 0.7 mm) of the size for the rib, to which the plate was stuck earlier, and at the expense of increase (from 0.2 mm to 1 mm) of the distance from the target surface to the heat carrier.

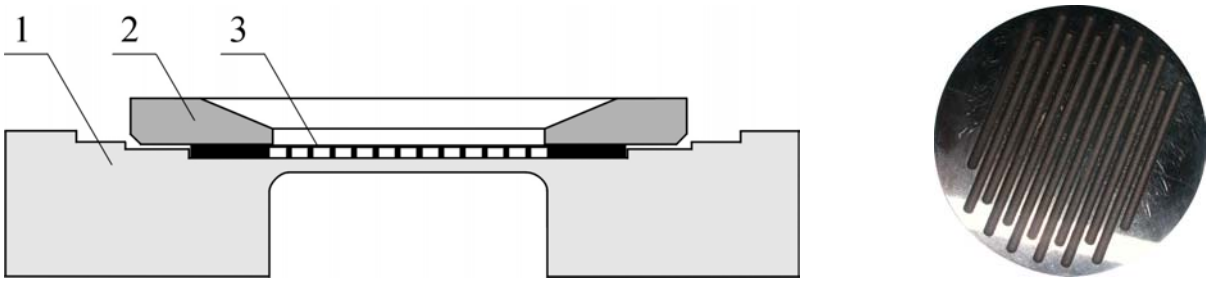

Fig. 1. Target. a) Target design: 1 – clamping flange, 2 – beam absorber (tungsten disk with 13 channels for cooling), 3 – titanium body. Proton beam falls onto the beam absorber from above. b) beam absorber photo; view from the side opposite the one which is exposed to the proton beam.

3. Hydrodynamic pressure drop

Turbulent flow of heat carrier in the channels provides effective cooling of the target. At steady rectilinear symmetric isothermal flow, hydrodynamic pressure drop ΔP is expressed by equation:

$$\Delta P = \zeta \frac{l}{d} \frac{\rho u^2}{2},$$

where ζ is hydraulic resistance, u – heat carrier velocity, l – channel length, d – characteristic transfer size of the channel ($d = 4\,S/\Pi$, S is the channel cross-sectional area, Π is its circumference), ρ – density. At turbulent flow in a plain tube, ζ may be well approximated in the region of Reynold's numbers $10^4 < Re = u\,d/\nu < 10^5$ (ν here is kinematic viscosity), that are characteristic for our case, by empiric formula:

$$\zeta = \frac{0.316}{Re^{0.25}}.$$

Hydraulic resistance of rough tubes ζ_r with mean height of lugs δ may be determined by approximate formula (Kutateladze, 1979):

$$\zeta_r = 0.11\left(\frac{\delta}{d} + \frac{68}{Re}\right)^{0.25}.$$

In addition to pressure drop in the cooling channels induced by friction, there is local hydraulic resistance inside the supplying system caused by hydraulic strikes at channel entrances, at sudden broadening of the channel's cross-section, at flow turn, junction or division, etc. (Idelchik, 1975). It was cleared out that the pressure drop in the supplying system for this prototype of the target exceeds the pressure drop in the channel induced by friction, and certainly requires minimizing. Evening-out the ell edges, curving the entrance channel walls, even change of cross-sections, etc. will allow to decrease essentially the pressure drop for the supplying system and to cool the target more efficiently.

4. Temperature drop between cooling surface and heat carrier

The main contribution into the temperature drop is made by the process of heat transfer from hard wall to the heat carrier through convective heat exchange. This temperature drop $\Delta T_{\text{w-liq}}$ is determined as

$$\Delta T_{\text{w-liq}} = P / \alpha S,$$

where P is the transferred heat power, S is heat exchange surface square, α is a heat transfer coefficient. α is defined as

$$\alpha = \frac{Nu\,\lambda}{d},$$

where Nu is the Nusselt criterion, λ – heat conductivity of heat carrier.

On the basis of influence of heat carrier characteristics on heat exchange conditions, all liquids may be divided into three main classes (Kutateladze, 1958) that are characterized by Prandtl criterion $Pr = \nu C_{\text{p}} \rho / \lambda$, where C_{p} – specific thermal capacity. These three classes are the following: liquids with $Pr \approx 1$, with $Pr > 1$, and with $Pr << 1$.

Nusselt criterion Nu for water characterized by the number Pr from 3 at 60 °C up to 8 at 20 °C, defined by empirical expression (Kutateladze, 1979):

$$Nu = \frac{0.023\,Pr\,Re^{0.8}}{1 + 2.14\,Re^{-0.1}\left(Pr^{2/3} - 1\right)}. \qquad (1)$$

Since $Pr > 1$ for water, and molecular transfer of momentum is more intense than molecular transfer of heat, the roughness of tube walls influences heat emission to turbulent flow. The roughness of the walls may be considered by introducing the additional factor of the ratio ζ_{r} of friction coefficient for rough tubes to the one of plain tubes:

$$Nu = \frac{0.023\left(\frac{\zeta_r}{\zeta}\right) Pr\,Re^{0.8}}{1 + 2.14\sqrt{\frac{\zeta_r}{\zeta}}\,Re^{-0.1}\left(Pr^{2/3} - 1\right)}. \qquad (2)$$

Heat transfer increases in rough tubes, but relatively weaker than hydraulic resistance factor.

To calculate heat transfer to gallium turbulent flow which is characterized $Pr = 0.0016$, Miheev-Bauman-Voskresensky-Fedinsky formula may be used (Kutateladze, 1979):

$$Nu = 3.4 + 0.014\,Pr^{0.8}\,Re^{0.8}.$$

Since heat transfer over heat conductivity channel for gallium is well more intense than molecular transfer of momentum, wall roughness does not effect heat emission.

5. Calculation of lithium layer temperature

Let us determine dependence of lithium layer temperature on heat carrier velocity at heat density q = 318 W cm^{-2} (which corresponds to 25 kW release on the target 10 cm in diameter).

The temperature of lithium layer T is evaluated as

$$T = \Delta T_{Li} + \Delta T_w + \Delta T_{w\text{-}liq} + \Delta T_{liq} + T_0,$$

where ΔT_w – temperature drop on lithium layer, ΔT_w – temperature drop on tungsten disk, $\Delta T_{w\text{-}liq}$ – temperature drop between the cooling surface and the heat carrier, determined above, ΔT_{liq} – mean heating of heat carrier, T_0 – initial heat carrier temperature.

The path of protons L with energy of 2 MeV in lithium medium is L = 270 μm, and tungsten medium L = 15 μm (Andersen, 1977).

The temperature drop on lithium is estimated as $\Delta T_{Li} = 0.5\, q_{Li}\, h_{Li} / \lambda_{Li}$, where coefficient 0.5 shows volumetric heat emission, lithium thickness is h_{Li} = 100 μm, power density released in lithium is $q_{Li} \sim q\, h_{Li}/L$, lithium heat conductivity is λ_{Li} = 43 W m^{-1} K^{-1}. In the case considered, ΔT_{Li} does not exceed 1 °C.

The path of proton in the target is obviously shorter of the order than the thickness of tungsten, therefore one can suppose in heat calculation that proton beam heats only the surface of tungsten disk. So, the temperature drop on disk is estimated as $\Delta T_w = q \cdot h_w / \lambda_w$, where thickness is h_w = 1 mm, tungsten heat conductivity is λ_w = 130 W m^{-1} K^{-1}. In this case ΔT_w = 25 °C.

Mean heat carrier heating ΔT_{liq}, which is determined to be equal to 1/2 of heat carrier heating on the way out of the system is insignificant for this target. At heat carrier velocity of u = 10 m s^{-1} ΔT_{liq} = 1 °C for water and ΔT_{liq} = 2 °C for gallium.

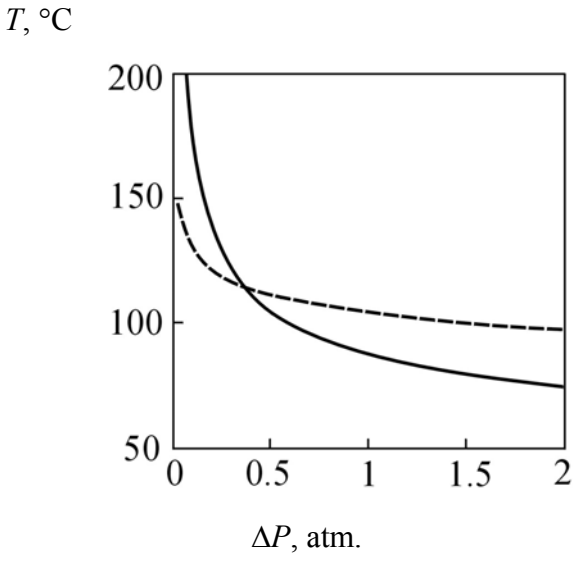

Fig. 2. Dependencies of lithium layer temperature for neutron producing target at pressure drop of heat carriers ΔP, that are 20 °C water (solid line), and 40 °C gallium (touch line), at 318 W cm^{-2} power density.

Temperature drop between the cooling surface and the heat carrier makes the main contribution into target heating. At u = 10 m s^{-1} the temperature drop for water $\Delta T_{w\text{-}liq}$ = 56 C° with initial temperature of water T_0 = 30 °C with wall roughness δ = 10 μm, and $\Delta T_{w\text{-}liq}$ = 30 °C for gallium. In Fig. 2, temperature dependencies for target surface on hydrodynamic pressure drop in

the channel for 20 °C water and for gallium with initial temperature $T_0 = 40$ °C are presented. The heat carrier velocity $u = 10$ m s^{-1} for water is realized at hydrodynamic pressure drop in channel $\Delta P = 0.4$ atm, and for gallium – 2.1 atm. This velocity in this target where all channels are paralleled results in heat carrier consumption of 2.8 m^3 hour^{-1}, which is quite high and may be reduced by series connection without noticeable rise in temperature.

It is clear that using water is possible and preferable for cooling of this target. This allows to refuse using gallium for cooling the target, therefore not to solve the problems of corrosion of target material and pump, arising from gallium influence.

6. Results of thermal experiment

Heat removal was studied using 20 kW heater. The heater is manufactured from nickel plate 1 mm thick, 45 mm × 45 mm, by cutting 2 mm stripes with 0.2 mm gap. The heater resistance is of order of 1 Ohm. It is pressed to the target through 1 mm thick BeO plate. The heater is fed from a stabilized power source with current up to 100 A. In Fig. 3, dependence of target surface temperature on heating is presented. 3 regimes of heat removal are seen: i) up to 250 W cm^{-2} – turbulent flow with good correlation to calculation, ii) with bubble boiling (temperature does not practically change when heating increases), and iii) with film boiling more then 450 W cm^{-2} (heat-transfer drops, and temperature increases sharply). Wide plate presenting allows to detect target overheating without this undesirable dropping of heat removal.

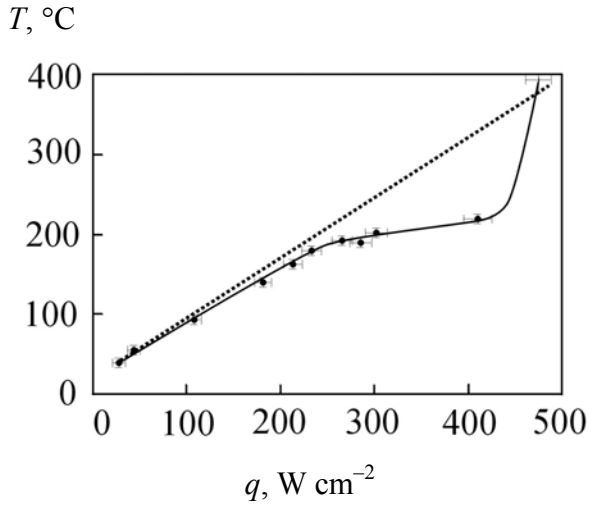

Fig. 3. Dependencies of target surface temperature at water velocity 3 m s^{-1} on heat density: solid line – measured, touch line – calculated.

7. Planned experiments and simulations for neutron target design

Radiation blistering is one of the main processes determining lifetime of a optimal target. Appearance of blisters results in increasing the lithium layer evaporation due to rise of temperature because of swelling and flaking. At current of 10 mA and target diameter of 10 cm, the upper bound of fluence in volume expansion and lower bound in blistering of 10^{17} cm^{-2} (Berish, 1983) is achieved during 130 s. Fluence of 10^{19} cm^{-2}, which certainly causes blistering is achieved during 3.5 hour. It is clear that the time of blister appearance is comparable to the time of planned radiation treatment. For different materials, fluence of blister appearance may differ due to difference in hydrogen diffusion coefficient. To determine the best target material, an experiment is planned in the near future to study hydrogen density distribution in depth for tungsten or copper beam absorber at its bombing with 40 kW, 50 keV, 2 s pulse proton beam. At choosing the material for target,

laboriousness of the electric-spark method for making cooling channels in tungsten will be taken into account. In this experiments, the target surface temperature will be determined by developed remote optic diagnostics.

8. Target design

Neutron producing target for the pilot neutron source under construction is proposed to correspond to the existing prototype with the following fundamental modifications: i) target diameter is to be increased up to 10 cm for 25 kW proton beam, ii) it will be cooled with water only, iii) to provide efficient cooling at minimal water consumption, the target channels are to be spiral, iv) thin lithium layer is to be evaporated immediately in the target unit. Calculation showed that the lithium target could run up to 10 mA proton beam before melting. The material for proton beam absorber is to be determined after planned experiments at the existing target prototype. Diagnostic equipment provides detecting α-particles inside the vacuum chamber close to the target and detecting neutrons and γ-rays outside.

9. Conclusion

Innovative accelerator based neutron source for neutron capture therapy is under construction now at the Budker Institute of Nuclear Physics. One of the main elements of the facility is lithium target producing neutrons via threshold ^{7}Li(p,n)^{7}Be reaction at 25 kW proton beam with energies 1.915 MeV or 2.5 MeV. Two neutron producing target prototypes were made and tested under powerful electron beam and heater. Hydraulic resistance for heat carrier flow in the target and lithium layer temperature were calculated. It became clear that using water is preferable for cooling this target, and that the lithium target could run up to 10 mA proton beam before melting. The material for proton beam absorber is to be determined after planned experiments on radiation blistering at the target prototype under available pulse proton beam. Neutron producing target design for the neutron source under construction is proposed.

Manufacturing the neutron producing target up to the end of 2004 and obtaining a neutron beam on BINP accelerator based neutron source are planned during 2005.

Acknowledgements

The authors would like to thank the financial support from International Science and Technology Center.

References

Andersen, H., 1977. Hydrogen stopping powers and ranges in all elements. Pergamon Press Inc.

Bayanov, B. *et al.*, 1998. Accelerator based neutron source for the neutron-capture and fast neutron therapy at hospital, Nucl. Instr. and Meth. in Phys. Res. A 413, pp. 397-426.

Belov, V. *et al.*, 2000. Neutron producing target for neutron capture therapy. Proc. 9th Intern. Symposium on Neutron Capture Therapy for Cancer, Osaka, Japan, pp. 253-254.

Belov, V. *et al*, 2002. Neutron producing target for accelerator based neutron source for NCT. Research and Development in Neutron Capture Therapy. Eds.: W. Sauerwein, R. Moss, and A. Wittig. Monduzzi Editore, pp. 247-252.

Berish, R. (Ed.), 1983. Sputtering by Particle Bombardment II. Springer-Verlag.

Idelchik, I., 1975. Hydraulic resistance reference book. Mashinostroenie, Moscow.

Kononov, O., Kononov, V., Soloviev, N., 2003. Near-threshold $^{7}Li(p,n)^{7}Be$ reaction based neutron source for boron neutron capture therapy. Atomic Energy, 94, pp. 469-472.

Kutateladze, S., *et al*, 1958. Liquid metal heat carrier. Atomizdat, Moscow.

Kutateladze, S., 1979. Heat transfer theory fundamentals. Atomizdat, Moscow. / E. Arnold Publishers, London, Academic Press Inc, New York, 1963.